Journal of Catalysis **206,** 114–124 (2002)
doi:10.1006/jcat.2001.3478, available online at http://www.idealibrary.com on IDEAL®

In Situ Fourier Transform Infrared Study of the Selective Reduction of NO with Propene over Ga_2O_3–Al_2O_3

Masaaki Haneda,*,†,‡,[1] Nicolas Bion,* Marco Daturi,* Jacques Saussey,* Jean-Claude Lavalley,* Daniel Duprez,† and Hideaki Hamada‡

*Laboratoire de Catalyse et Spectrochimie, UMR CNRS-ISMRA 6506, 6 Bd du Maréchal Juin, F-14050 Caen Cedex, France; †Laboratoire de Catalyse en Chimie Organique (LACCO), UMR CNRS 6503, Université de Poitiers, 40 Avenue du Recteur Pineau, 86022 Poitiers Cedex, France; and ‡National Institute of Advanced Industrial Science and Technology (AIST), AIST Tsukuba Central 5, 1-1-1 Higashi, Tsukuba, Ibaraki 305-8565, Japan

Received August 9, 2001; revised October 22, 2001; accepted November 15, 2001; published online January 14, 2002

The selective reduction of NO with propene has been investigated on Al_2O_3 and Ga_2O_3–Al_2O_3, using *in situ* diffuse reflectance Fourier transform infrared (FT–IR) spectroscopy combined with on-line mass spectrometry and IR gas analysis. During the NO–C_3H_6–O_2 reaction, the main surface species detectable by IR were adsorbed nitrate, acetate, formate, cyanide (–CN), and isocyanate (–NCO). Ga_2O_3 was found to promote the formation of these surface species, especially nitrate, –CN, and –NCO. From the experiments focusing on the reactivity of surface NO_x(ads) (nitrite and nitrate) species, we found a very high reactivity of those compounds toward C_3H_6, leading to the rapid formation of –CN and –NCO species. On the other hand, acetate and formate species were deduced to be spectator species in this reaction. An appearance of ν(NH) bands ascribed to the formation of the surface complexes including amido groups (–NH complexes) was observed simultaneously with a decrease of the –NCO band, suggesting that the –NCO species is hydrolyzed to the –NH complexes by the reaction with some traces of water. A reaction mechanism has been proposed: NO_x(ads) species formed by NO–O_2 reaction on the catalyst surface react with C_3H_6-derived species to generate the –NCO species via acrylic species and organic nitro compounds, and then the surface –NH complexes generated by hydrolysis of the –NCO species react with NO_x(ads) species or NO_2 to produce N_2. © 2002 Elsevier Science (USA)

Key Words: **selective reduction of NO; *in situ* diffuse reflectance FT–IR; Ga_2O_3–Al_2O_3; reaction mechanism.**

1. INTRODUCTION

Since the report of Cu-ZSM-5 by Held *et al.* (1) and Iwamoto *et al.* (2), the selective catalytic reduction (SCR) of nitrogen oxides (NO_x) by hydrocarbons (HC-SCR) currently attracts great interest in both applied and fundamental research. From the extensive investigations thus far, not only metal ion-exchanged zeolites (3–10) but also metal oxide-based catalysts (9–15) were found to catalyze the NO reduction by hydrocarbons or oxygenated hydrocarbons. Among them, alumina-supported metal (oxide) catalysts will be promising candidates for practical applications because of their high stability.

Many different reaction mechanisms for HC-SCR have been proposed and can be roughly classified as "decomposition" and "reduction" mechanisms (10, 11). The latter mechanism in which NO is reduced into N_2 via some nitrogen- and oxygen-containing intermediates has been supported by many researchers (16–20). However, it seems that there are some disagreements in the literature regarding the reaction pathway. In recent infrared (IR) studies, NO_x(ads) species such as nitrates (NO_3^-) on oxide catalysts resulting from the oxidation of NO played an important role as the initial intermediate in NO reduction by hydrocarbons (21–25). In addition, Shimizu *et al.* (24, 26) reported that surface acetate species formed on Al_2O_3 through the oxidation of C_3H_6 would participate in N_2 formation by the reaction of surface nitrate species. On the other hand, the possibility of isocyanate species (27–31) and ammonia (32–34) as the final intermediates has been proposed by many researchers. It is extremely important to examine the role and reactivity of the intermediates formed in each reaction step for the reaction mechanistic study. However, little detailed work with respect to the behavior of a series of intermediates formed through the reaction has been performed.

The present paper is devoted to the systematic *in situ* diffuse reflectance FT–IR study on the formation and reaction of adsorbed species in NO reduction by propene over Ga_2O_3–Al_2O_3. The transient and pulse reaction techniques followed by IR and mass spectroscopic (MS) analysis were employed to examine the reactivity and dynamic behavior of surface species. In particular, the reactivity of surface NO_x(ads) (NO_2^- and NO_3^-) species with propene was the focus of our study, because of the importance of surface NO_x(ads) species in this reaction from kinetic studies (35). A proposed reaction mechanism

[1] To whom correspondence should be addressed at the National Institute of Advanced Industrial Science and Technology, AIST Tsukuba Central 5, 1-1-1 Higashi, Tsukuba, Ibaraki 305-8565, Japan. Fax: 81-298-61-4647, E-mail: m.haneda@aist.go.jp.

0021-9517/02 $35.00

based on this *in situ* diffuse reflectance FT–IR study is discussed.

2. EXPERIMENTAL

Ga_2O_3–Al_2O_3 catalyst was prepared by the sol–gel method. Aluminum boehmite sol was first prepared by hydrolyzing aluminum(III) triisopropoxide in hot water (363 K) with a small amount of nitric acid, and then by mixing it with a solution of gallium(III) nitrate dissolved in ethylene glycol. After the solution was stirred at room temperature for 1 day, the solvents were eliminated by heating under reduced pressure. The resulting catalyst precursor was dried at 383 K, followed by calcination at 873 K for 5 h in flowing air. The loading of gallium oxide, calculated as Ga_2O_3, was fixed at 30 wt%. Alumina was also synthesized from aluminum boehmite sol as described earlier. After the sol solution was heated under reduced pressure to remove the solvents, the residue was dried at 383 K and calcined at 873 K for 5 h in flowing air. The BET surface areas of Al_2O_3 and Ga_2O_3–Al_2O_3 were 207 and 191 $m^2\ g^{-1}$, respectively.

For the diffuse reflectance FT–IR measurements, the catalyst powder (20 mg) was placed in a diffuse reflectance high-temperature cell (Spectra Tech) fitted with KBr windows. IR spectra were recorded with a Nicolet 550 FT–IR spectrometer, accumulating 64 scans at a resolution of 4 cm^{-1}. Gas products were analyzed by a quadrupole mass spectrometer (QMS, Balzers TCP 121) and by FT–IR in a gas microcell with a volume of 0.088 cm^3. Prior to each experiment, the catalyst was activated *in situ* by heating in a flow of 10% O_2/Ar at 873 K, followed by cooling to the desired temperature and correcting the spectrum of the clean surface which was used as a background. Various gas mixtures were fed to the catalyst at a flow rate of 25 $cm^3\ min^{-1}$. The concentrations of NO, C_3H_6, and O_2 in the gas mixture were 1000 ppm, 1000 ppm, and 10% with Ar balance, respectively. The identification of surface species was carried out under steady-state conditions as the reaction temperature was changed from 523 to 723 K in steps of 50 K. The IR spectra were taken in 45 min at a given temperature.

In addition to the steady-state reaction, a transient reaction technique was employed to clarify the role and reactivity of surface species. The catalyst was first exposed to either C_3H_6/O_2/Ar or NO/O_2/Ar at 623 K for 90 min to form and accumulate the surface species. After purging in Ar for 10 min, the reaction gas was switched to various gas mixtures, and then changes in the intensity of IR bands were measured with time on stream. We also performed a pulse reaction to examine in detail the reactivity of surface NO_x(ads) species. The catalyst was exposed to NO/O_2/Ar until the concentration of surface NO_x(ads) species reached the steady state, and then five consecutive pulses of C_3H_6 (volume of one pulse: 20 μL) were injected into the steady-state flow of NO/O_2/Ar at 573, 623, 673, and 723 K. Changes in the intensity of IR bands due to the surface species and gaseous products were measured with time on stream.

3. RESULTS

3.1. Surface Species Formed in a Flow of Various Gas Mixtures

Figure 1 shows the IR spectra of adsorbed species formed on Al_2O_3 and Ga_2O_3–Al_2O_3 in various flowing gas mixtures at 573 K. In flowing NO/Ar (spectra a and b), a weak IR band assignable to the ν_3 split stretching vibration mode of free nitrite (NO_2^-) species (36, 37) was detected at 1232 cm^{-1} for both catalysts. When the catalyst was exposed to NO/O_2/Ar (spectra c and d), more intense IR bands compared to those in NO/Ar at 1234, 1291, 1560, and 1584 cm^{-1} were observed. It was reported that nitrate (NO_3^-) species on the metal oxides gives two bands at 1650–1500 and 1170–1300 cm^{-1} in the region, assigned to the ν_3 split stretching vibration (36, 37). The two bands observed here were assigned to monodentate (1560 and 1234 cm^{-1}) and bidentate (1584 and 1291 cm^{-1}) NO_3^- species. No great difference in the position of the NO_3^- bands was observed between Al_2O_3 and Ga_2O_3–Al_2O_3. This is probably due to the presence of a composite oxide represented by $[Ga_xAl_{(1-x)}]_2O_3$ ($x < 1$) in Ga_2O_3–Al_2O_3 (35), leading to the difficulty in distinguishing the adsorption sites of NO_3^-, Ga^{3+}, and/or Al^{3+}. On the other hand, the intensity of the bands assignable to the NO_3^- species is greater for Ga_2O_3–Al_2O_3 than for Al_2O_3, indicating that the surface of Ga_2O_3–Al_2O_3 is very reactive for the oxidation of NO_x to NO_3^-. A detailed discussion will be made afterwards. Conversely, the result cannot be justified

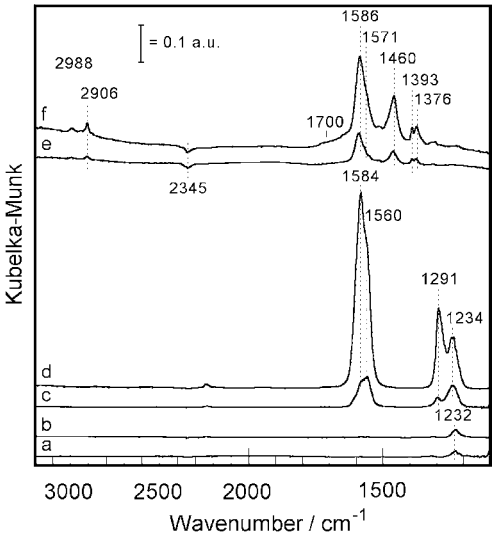

FIG. 1. Diffuse reflectance FT–IR spectra of adsorbed species on Al_2O_3 (a, c, e) and on Ga_2O_3–Al_2O_3 (b, d, f). The spectra were taken in flowing (a, b) NO (1000 ppm)/Ar for 60 min, (c, d) NO (1000 ppm)/O_2 (10%)/Ar, and (e, f) C_3H_6 (1000 ppm)/O_2 (10%)/Ar at 573 K for 45 min.

by differences in surface basicity, since we know that it is the same for both samples (38).

In flowing $C_3H_6/O_2/Ar$ (spectra e and f), two strong bands at about 1460 and 1586 cm^{-1} with a shoulder band at 1571 cm^{-1} and two weak bands at 1376 and 1393 cm^{-1} were observed for both catalysts. The bands at 1460 and 1571 cm^{-1} were assigned to $\nu_s(COO^-)$ and $\nu_{as}(COO^-)$ stretches of adsorbed acetate species, respectively, because their frequencies were in good agreement with those of acetic acid adsorbed on alumina (24, 39). The other three bands were in agreement with those observed in previous studies showing formates adsorbed on alumina (24, 40). Hence, the bands at 1586, 1393, and 1376 cm^{-1} were assigned to $\nu_{as}(COO^-)$, $\delta(CH)$, and $\nu_s(COO^-)$ of adsorbed formate species, respectively. This assignment is also supported by the small absorption bands in the C–H stretching region (between 2900 and 3000 cm^{-1}). A broad IR band at 1700 cm^{-1}, which is ascribed to carbonyl (>C=O) species (37, 41), also appeared for Ga_2O_3–Al_2O_3. With respect to the background spectrum, the features at around 2350 cm^{-1} are ascribed to an imperfect subtraction of CO_2 traces in the small dead volume of the cell and/or in the optical bench. It should be noted that no great difference in the features of the IR spectra, except for the band intensity, was observed between Al_2O_3 and Ga_2O_3–Al_2O_3. In agreement with our reaction data (35), Ga_2O_3 seems to effectively promote C_3H_6 oxidation but not to affect the nature of the adsorption sites for acetate and formate species.

3.2. Formation of Adsorbed Species during SCR Reaction

3.2.1. Effect of reaction temperature. The IR spectra recorded during the NO–C_3H_6–O_2 reaction over Al_2O_3 and Ga_2O_3–Al_2O_3 in the temperature range between 523 and 723 K are shown in Figs. 2 and 3, respectively. For both

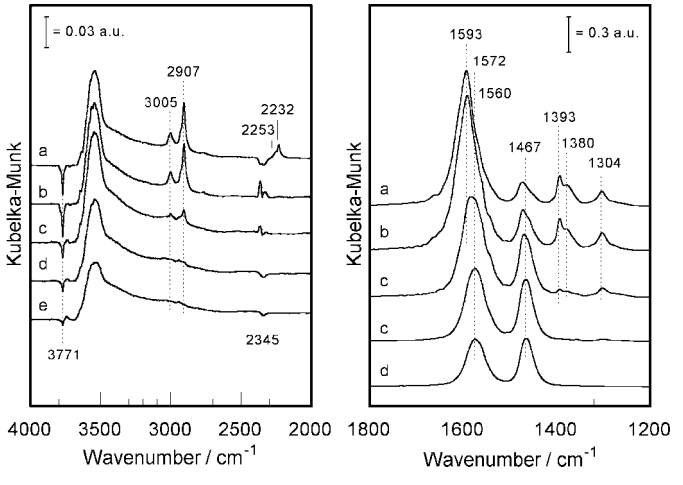

FIG. 2. Diffuse reflectance FT–IR spectra of adsorbed species in flowing NO (1000 ppm)/C_3H_6 (1000 ppm)/O_2 (10%)/Ar on Al_2O_3 at (a) 523, (b) 573, (c) 623, (d) 673, and (e) 723 K for 45 min.

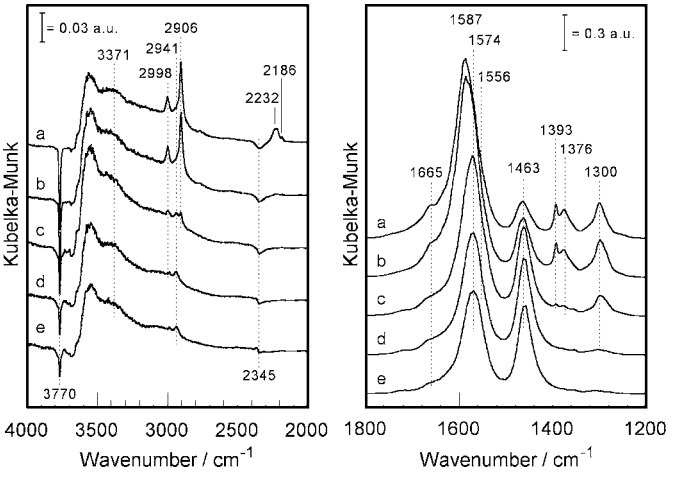

FIG. 3. Diffuse reflectance FT–IR spectra of adsorbed species in flowing NO (1000 ppm)/C_3H_6 (1000 ppm)/O_2 (10%)/Ar on Ga_2O_3–Al_2O_3 at (a) 523, (b) 573, (c) 623, (d) 673, and (e) 723 K for 45 min.

catalysts, it appears that the bands detected in the spectral range below 1800 cm^{-1} are almost the same as those observed in flowing $NO/O_2/Ar$ and $C_3H_6/O_2/Ar$ (Fig. 1): NO_3^- (1300 and shoulder ~1574 cm^{-1}), formate (1376, 1393, and 1587 cm^{-1}), and acetate (1463 and 1574 cm^{-1}) species. Relevant band assignments are listed in Table 1. Interestingly, acetate and formate species already appear at 473 K (523 K in the $C_3H_6/O_2/Ar$ flow, results not shown), indicating that the presence of NO in the stream improves hydrocarbon oxidation. Obviously, no great difference in the IR spectra below 1800 cm^{-1} was observed between Al_2O_3 and Ga_2O_3–Al_2O_3. The slight difference is that a broad IR band at 1665 cm^{-1} was detected on the latter catalyst. Although this band is ascribed to bridging NO_3^- species in which the IR band appears at around 1600–1650 cm^{-1} (36, 37), its band frequency is too high compared to that reported on Al_2O_3 (1615 cm^{-1}) (23). The fact that this band was not observed in flowing $NO/O_2/Ar$ and $C_3H_6/O_2/Ar$ makes it possible to assume that it is due to organic compounds including nitrogen and oxygen atoms. In the literature (43–45), the IR absorption band ascribed to the organic nitrito (R-ONO) compound appears at around 1655 cm^{-1}. Taking into account the weak bands at around 3371 cm^{-1} (ν(NH) stretching vibrations) which evolve in the same way, this feature is also likely due to the ν(CO) vibration of acrylamide species (46, 47).

In the region above 2000 cm^{-1}, the bands assignable to the ν(CH) vibration mode of adsorbed formate species were observed at ca. 2906 cm^{-1}, while the feature at ~3000 cm^{-1} was an overtone due to $\nu_{as}(COO^-) + \delta(CH)$ modes (40). The band at 2941 cm^{-1} observed at 723 K was assigned to the ν(CH) vibration mode of adsorbed acetate species (48). No IR bands at 2300–2400 cm^{-1}, confirming the formation of CO_2 in the region, were observed at any reaction temperature, due to the small volume occupied by

TABLE 1

Wavenumber and Assignment of Absorption Bands in Diffuse Reflectance FT–IR Spectra

Wavenumber/cm^{-1}	Surface species	Interpretation	References
1232	Nitrite (NO_2^-)	ν_{as}(ONO)	36, 37
1560	Monodentate nitrate (NO_3^-)	ν(N=O)	36, 37
1234		ν_{as}(ONO)	
1584	Bidentate nitrate (NO_3^-)	ν N=O)	36, 37
1291		ν_{as}(ONO)	
2941	Acetate	ν(CH)	24, 39, 48
1571		ν_{as}(COO$^-$)	
1460		ν_s(COO$^-$)	
2997	Formate	ν_{as}(COO$^-$) + δ(CH)	24, 40
2906		ν(CH)	
2924[a]		ν(CH)	40
2860[a]			
1586		ν_{as}(COO$^-$)	
1393		δ(CH)	
1376		ν_s(COO$^-$)	
3094	Acrylic species?	$\nu(CH_2)$	47
1700	Carbonyl (>C=O)	ν(CO)	37, 41
1665	Acrylamide?	ν(CO)	46, 47
2253	Isocyanate –NCO	ν(N=C=O)	49–51
2232			
2186	Cyanide –CN	ν(C≡N)	51, 52
3382	–NH compounds (acrylamide?)	ν(NH)	32, 33, 37
3398			

[a] The bands are assigned to a Fermi resonance between the ν(CH) fundamental and a combination band of the same symmetry.

the gas above the catalyst surface in the reactor cell and probably because the CO_2 bands as the reaction product were counteracted by those decreasing with time in the optical path. In fact, the simultaneous gas analysis by FT–IR confirmed the formation of CO_2, whose amount increased with reaction temperature. In agreement with the reaction data (35), the amount of CO_2 formed on Ga_2O_3–Al_2O_3 was much greater than that formed on Al_2O_3.

In addition to these bands, a distinct IR band at 2232 cm^{-1} with a shoulder at 2253 cm^{-1} was observed during the reaction over Al_2O_3 at 473 K (Fig. 2 (a)). Since the frequency of these bands is very similar to that of the band observed on Al_2O_3 by Ukisu *et al.* (49, 50), the bands at 2232 and 2253 cm^{-1} were assigned to isocyanate (–NCO) species formed on two different Al^{3+} sites (coordinatively unsaturated (*cus*) tetrahedral and octahedral Al^{3+}) (51). On the other hand, in Ga_2O_3–Al_2O_3, similar IR bands appeared at ~2250 and 2232 cm^{-1} (the former perturbed by CO_2 traces features) during the reaction at 473 K (Fig. 3 (a)), with an additional component at 2186 cm^{-1}. This latter band can be assigned to surface cyanide (–CN) species (51). The intensity of the –NCO band was slightly stronger for Ga_2O_3–Al_2O_3 than for Al_2O_3, suggesting that Ga_2O_3 accelerates the formation of –NCO species. It is noteworthy that the –CN and –NCO bands on both catalysts totally disappear above 573 K.

3.2.2. Time dependence. Our previous catalytic experiments established that NO reduction into N_2 over Ga_2O_3–Al_2O_3 was effectively catalyzed at the temperatures above 623 K (35). To clarify the behavior of surface species formed at the initial stage of the reaction, the time-dependent changes of surface species formed during the NO–C_3H_6–O_2 reaction over Ga_2O_3–Al_2O_3 at 623 K were measured. As shown in Fig. 4, the formation of formate (1377, 1393, and 1590 cm^{-1}) and acetate (1460 and 1576 cm^{-1}) species was observed immediately after the gas introduction. Although the formation of NO_3^- species was also recognized during the reaction, their behavior differs depending upon the adsorption structure. Namely, monodentate NO_3^- species (1554 cm^{-1}) were initially formed, while bidentate NO_3^- species (characterized by the band at 1300 cm^{-1}, which is the parent band at higher wavenumbers superimposed to acetate features) were detected only after an induction period of ca. 30 min. This may be due to the difference in the reactivity toward the other gases such as C_3H_6. Interestingly, a rapid build-up intensity of the features attributed to the –CN (2165 cm^{-1}) and –NCO (2244 cm^{-1}) species was observed in the first 5 min, even though these peaks could not be detected during the steady-state reaction (Fig. 3 (c) left and right panels). The integrated area of the band for –CN and –NCO reached a maximum after 150 and 120 s, respectively, followed by a slow decrease (results not shown). This is consistent with previous reports in which the –NCO species were formed very quickly on Rh/Al_2O_3 (52), Pt/Al_2O_3 (52, 53), and Ag/Al_2O_3 (23). It should be noted that the –CN and –NCO bands completely

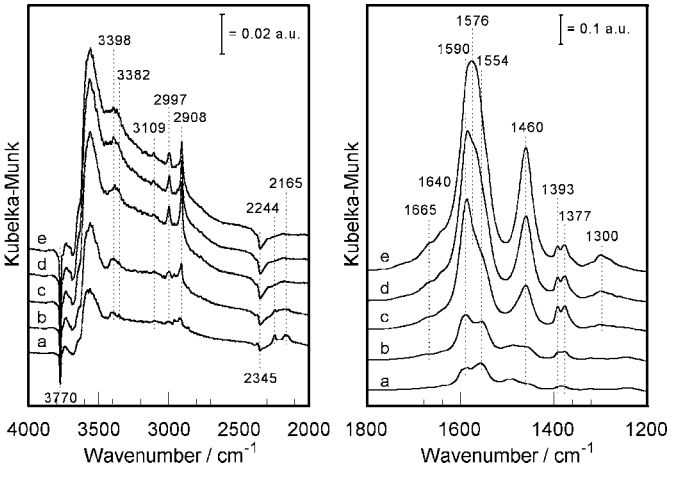

FIG. 4. Diffuse reflectance FT–IR spectra of adsorbed species in flowing NO (1000 ppm)/C_3H_6 (1000 ppm)/O_2 (10%)/Ar on Ga_2O_3–Al_2O_3 at 623 K as a function of reaction time: (a) 5, (b) 10, (c) 30, (d) 60, and (e) 90 min.

disappeared 10 min after the reaction started (Fig. 4 (b) left and right panels), suggesting that these species were highly reactive toward the reaction gases.

As can be seen in Fig. 4, it is noteworthy that weak IR bands were observed at around 3382 and 3398 cm^{-1} during the reaction at 623 K. Their wavenumber is characteristic of NH vibrations (32, 33, 37). To specify such an assignment, Ga_2O_3–Al_2O_3 was exposed to NH_3 pulsing (20 μL) in flowing Ar at 623 K. Three bands assignable to the ν(NH) stretching mode of adsorbed ammonia at 3392, 3338, and 3288 cm^{-1} along with those of $\delta(NH_3)$ vibration of NH_3 coordinated to Al^{3+} and/or Ga^{3+} at 1264 and 1279 cm^{-1} were observed (results not shown). The latter two bands were not recognized in the IR spectra taken during the NO–C_3H_6–O_2 reaction, and the former are at significantly different wavenumbers (Fig. 4). Thus, the IR bands near 3398, 3382, and 1665 cm^{-1} might be assigned to the compounds including amino groups such as ammonia and amines and/or amido groups such as acrylamide (or acetamide) as cited earlier. In the acrylamide assignment, the presence of the band at 1665 cm^{-1} is prefered (47). The fact that the ν(NH) bands did not appear during the reaction on Al_2O_3 (Fig. 2) suggests that Ga_2O_3 plays an important role in the formation and/or coordination of –NH compounds.

3.3. Reactivity of Surface Oxygenate (Acetate and Formate) Species

Figure 5 shows the changes in the integrated areas of the bands due to acetate (1405–1504 cm^{-1}) and formate (1365–1405 cm^{-1}) species with time on stream during the C_3H_6–O_2 reaction over Al_2O_3 and Ga_2O_3–Al_2O_3 at 623 K (left side of the figure), followed by Ar purging for 10 min and by switching flowing gas to Ar, O_2/Ar, or NO/O_2/Ar (right side of the figure). As described previously, the formation of acetate and formate species seems to be remarkably promoted by the presence of Ga_2O_3. When the reaction gas was switched to either Ar or O_2/Ar, no considerable decrease in the intensity of acetate and formate was observed, indicating that these species were stable in an inert gas and O_2. In contrast, the bands due to acetate and formate species significantly decreased in flowing NO/O_2/Ar.

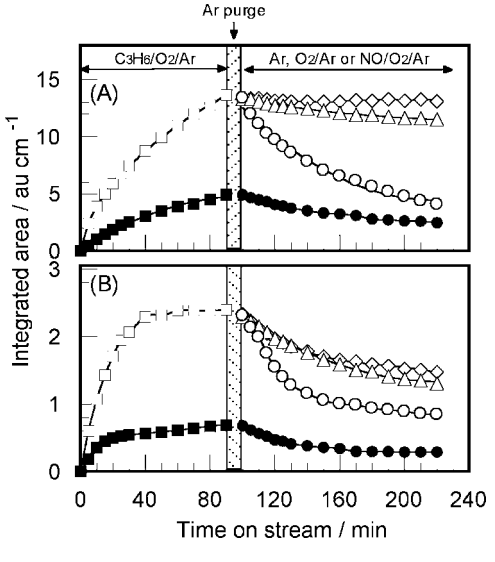

FIG. 5. Time dependence of the integrated area of the bands due to (A) acetate (1405–1504 cm^{-1}) and (B) formate (1365–1405 cm^{-1}) species formed during the reaction of C_3H_6 (1000 ppm)/O_2 (10%)/Ar (■, □) on Al_2O_3 and Ga_2O_3–Al_2O_3 at 623 K, followed by Ar purge for 10 min and switching flowing gas to Ar (◇), O_2(△), or NO + O_2 (●, ○). Closed symbols (■, ●) indicate the results for Al_2O_3, and open ones indicate results (□, ◇, △, ○) for Ga_2O_3–Al_2O_3.

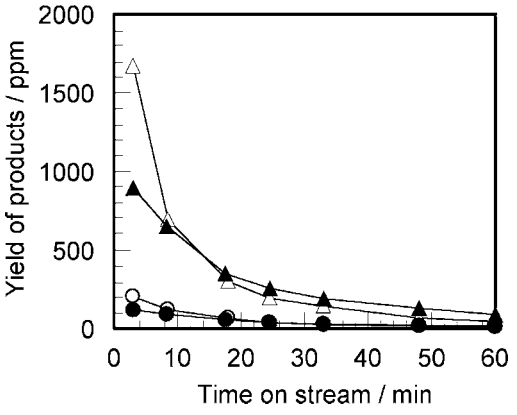

FIG. 6. Time dependence of the yield of N_2 (●, ○) and CO_x (CO + CO_2, ▲, △) formed by the reaction of oxygenate (acetate and formate) species with NO/O_2 on Al_2O_3 (●, ▲) and Ga_2O_3–Al_2O_3 (○, △) at 623 K. Oxygenate species were produced by exposing C_3H_6 (900 ppm)/O_2 (10%)/He to the catalysts (0.5 g) at 623 K for 5 h, followed by He purge for 30 min and switching flowing gas to NO (900 ppm)/O_2 (10%)/He.

Here, two possibilities concerning the decrease in the intensity of the bands can be presumed: reaction with NO/O_2 or site competition with another species (e.g., NO_3^-). If the first possibility occurs, the formation of some compounds including "N," "C," and "O" atoms is expected. However, no IR bands assignable to the compounds including "N," "C," and "O" atoms such as –NCO and –CN were detected (results not shown). Only the IR bands at 1246 and 1295 cm^{-1} due to NO_x(ads) species (NO_2^- and NO_3^-) were observed and their intensities increased with reaction time, suggesting that NO_x(ads) species and acetate/formate species may be competitively adsorbed on the same sites. On the other hand, in another set of experiments, the formation of a small amount of N_2, compared to CO_x (CO + CO_2), was recognized in the reaction of oxygenate species and NO/O_2 (Fig. 6), where the experiment was carried out as follows: 0.5 g of the catalyst was first exposed to C_3H_6 (900 ppm)/O_2 (10%)/He at 623 K for 5 h to accumulate oxygenate species on the surface, and then the reaction gas mixture was switched to NO (900 ppm)/O_2 (10%)/He. Some of the oxygenate species seem to be capable of reacting with NO_x (NO_2 and/or NO_x(ads)) to

form N_2. It should be noted that no great difference in the yield of N_2 and CO_x was observed between Ga_2O_3–Al_2O_3 and Al_2O_3 (Fig. 6), suggesting that this reaction proceeded mainly on Al_2O_3.

3.4. Reactivity of Surface NO_x(ads) Species

3.4.1. Transient reaction. Figure 7 shows the changes in the surface concentration of NO_x(ads) species, which were estimated from the correlation between the amount of adsorbed NO_x species and the integrated area of the bands due to NO_x(ads) species, with time on stream during the NO–O_2 reaction over Al_2O_3 and Ga_2O_3–Al_2O_3 at 623 K (left side of the figure). In a series of experiments, the evolution of NO_2^- and NO_3^- species (abbreviated as NO_x(ads) species) versus time was considered to be difficult in separating the two contributions by integrating the area of the bands in the region 1175–1335 cm^{-1}. It appears that the surface concentration of NO_x(ads) species linearly increased with reaction time up to 30 min. The initial formation rate of NO_x(ads) species determined from the slope of this line was 1.56×10^{-6} mol g^{-1} min^{-1} for Al_2O_3 and 2.52×10^{-6} mol g^{-1} min^{-1} for Ga_2O_3–Al_2O_3. The formation rate of NO_x(ads) species was found to be least 1.6 times faster on Ga_2O_3–Al_2O_3 than on Al_2O_3.

The reactivity of NO_x(ads) species toward C_3H_6 was evaluated by the transient response of the IR spectra at 623 K. As shown in Fig. 7 (right side), NO_x(ads) species seem to be stable in an inert gas such as Ar. In contrast, the surface concentration of NO_x(ads) species significantly decreased in C_3H_6/Ar or C_3H_6/O_2/Ar, indicating that NO_x(ads) species were reactive toward C_3H_6. The fact that no great difference in the apparent consumption rate of

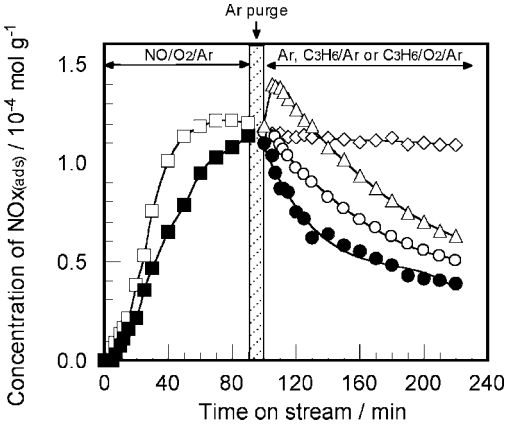

FIG. 7. Time dependence of the surface concentration of NO_x adspecies (NO_2^- and NO_3^-, 1175–1335 cm^{-1}) formed during the reaction of NO (1000 ppm)/O_2 (10%)/Ar (■, □) on Al_2O_3 and Ga_2O_3–Al_2O_3 at 623 K, followed by Ar purge for 10 min and switching flowing gas to Ar (◇), C_3H_6 (1000 ppm)/Ar (●, ○), or C_3H_6 (1000 ppm)/O_2 (10%)/Ar (△). Closed symbols (■, ●) indicate the results for Al_2O_3, and open ones (□, ◇, ○, △) indicate results for Ga_2O_3–Al_2O_3.

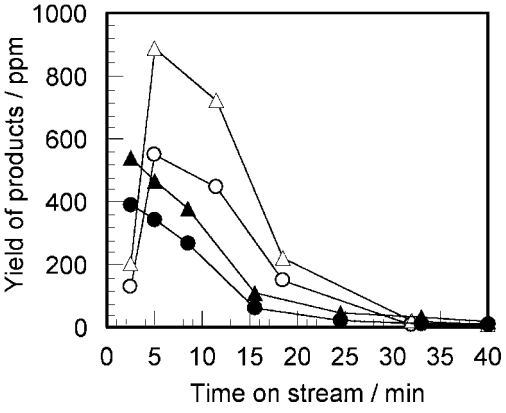

FIG. 8. Time dependence of the yield of N_2 (●, ○) and CO_x ($CO + CO_2$, ▲, △) formed by the reaction of NO_x adspecies with propene on Al_2O_3 (●, ▲) and Ga_2O_3–Al_2O_3 (○, △) at 623 K. NO_x adspecies were produced by exposing NO (900 ppm)/O_2 (10%)/He to the catalysts (0.5 g) at 623 K for 5 h, followed by He purge for 30 min and switching flowing gas to C_3H_6 (900 ppm)/He.

NO_x(ads) species was observed between the reaction with C_3H_6 and that with C_3H_6/O_2 suggests that O_2 does not significantly promote the reaction between NO_x(ads) species and C_3H_6. Interestingly, when the reaction gas was switched to C_3H_6/O_2/Ar, an increase in the intensity of the IR bands due to NO_x(ads) species was observed. This might be due to the formation of acetate species by C_3H_6–O_2 reaction, because weak IR bands assignable to acetate species appear in the region at 1200–1235 and 1290–1340 cm^{-1} (24, 48). It should be pointed out that the apparent consumption rate of NO_3^- species by the reaction with C_3H_6 over Al_2O_3 was very similar to that over Ga_2O_3–Al_2O_3, suggesting that this reaction proceeded mainly on Al^{3+} sites.

Figure 8 shows the results of another set of experiments to determine the yield of products for the reaction of NO_x(ads) and C_3H_6. The catalyst, 0.5 g, was first exposed to NO (900 ppm)/O_2 (10%)/He at 623 K for 5 h to accumulate NO_x(ads) species on the surface, and then the reaction gas mixture was switched to C_3H_6 (900 ppm)/He. Interestingly, quite different behavior in the formation of N_2 and CO_x ($CO + CO_2$) was observed between Al_2O_3 and Ga_2O_3–Al_2O_3. The yield of N_2 and CO_x on Ga_2O_3–Al_2O_3 first increased with time, passed through a maximum at 5 min, and then decreased, while that on Al_2O_3 monotonically decreased with time. The yield of N_2 and CO_x over Ga_2O_3–Al_2O_3 was found to be much larger than that on Al_2O_3, although the amount of NO_x adsorption evaluated in another set of experiments was almost the same for both catalysts (ca. 1.2×10^{-4} mol-NO g-cat^{-1}).

Figure 9 shows the changes in the IR spectra of adsorbed species on Ga_2O_3–Al_2O_3 as a function of time after the reaction gas was switched to C_3H_6. In the spectral range below 1800 cm^{-1}, it appears that a consumption of NO_x(ads) species (1335–1175 cm^{-1}) and a buildup of

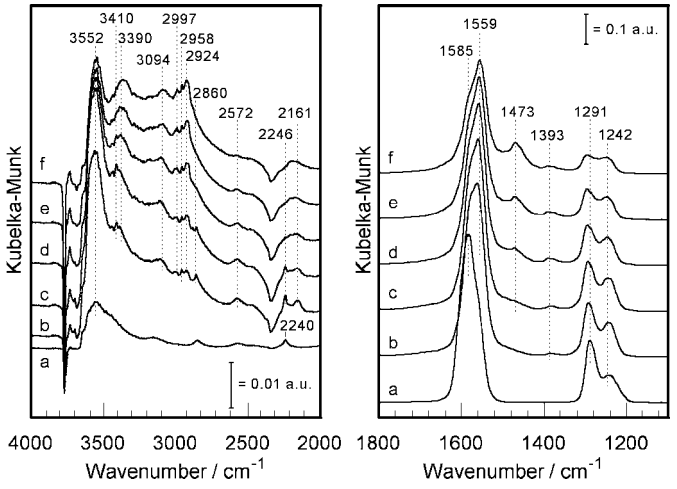

FIG. 9. Diffuse reflectance FT–IR spectra of adsorbed species on Ga_2O_3–Al_2O_3 at 623 K. The spectra were taken in flowing NO (1000 ppm)/O_2 (10%)/Ar at 623 K for 90 min, followed by Ar purge for 10 min and switching flowing gas to C_3H_6 (1000 pm)/Ar for (a) 0, (b) 5, (c) 10, (d) 30, (e) 60, and (f) 120 min.

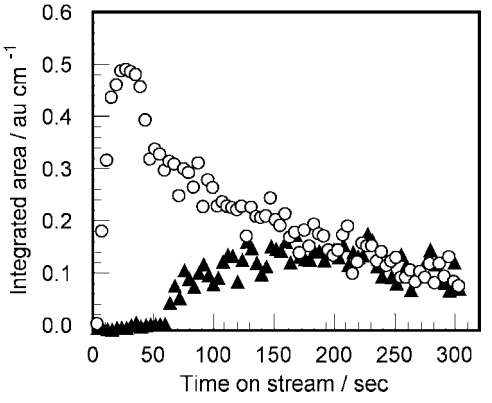

FIG. 10. Time dependence of the integrated area of the bands for –CN (▲, 2110–2192 cm^{-1}) and –NCO (○, 2205–2295 cm^{-1}) species formed during the reaction between NO_x(ads) species (NO_2^- and NO_3^-) and C_3H_6 on Ga_2O_3–Al_2O_3 at 623 K.

acetate (1473 cm^{-1}) and formate (1393 cm^{-1}) species take place simultaneously, suggesting that the reaction of NO_x(ads) species and C_3H_6 leads to the formation of acetate and formate species, which can be competitively adsorbed on the sites liberated by the NO_x(ads) compounds. A rapid buildup of acetate and formate species was also observed in the region of the C–H stretching vibration modes (2850–3000 cm^{-1}), whose band intensities increased with the reaction time. It should be noted that a new IR band at 3094 cm^{-1}, which can be assigned to the $\nu(CH_2)$ stretching vibration of acrylic species (46), was detected. These results suggest that the reaction of NO_x(ads) with C_3H_6 leads to the formation of acetate, formate, and acrylic species.

In the spectral range above 2000 cm^{-1}, additional IR bands assignable to –CN (2146 cm^{-1}) and –NCO (2246 cm^{-1}) species appeared immediately after the reaction gas was switched to C_3H_6 or C_3H_6/O_2, although in the latter reaction their band intensities were weaker than those in the former reaction. As shown in Fig. 10, the formation rate of the –NCO species is quite fast and its amount reaches a maximum in ca. 25 s, while the –CN band was detected with a 60-s induction period. This fact suggests that the formation rate of –CN and –NCO is fast and that both species are formed through alternative routes. It is of interest that an appearance of IR bands in the N–H stretching region (3390 and 3410 cm^{-1}) was recognized parallel to a disappearance of the –NCO band in the transient reaction of NO_x(ads) species with C_3H_6 (Fig. 9). The band intensity increased gradually with the reaction time. On the other hand, in agreement with the results of the steady-state reaction (Fig. 2), no distinct peaks assignable to the ν(NH) stretch were observed during the reaction over Al_2O_3 (results not shown). Let us recall that Ga_2O_3 promotes the formation of surface compounds including amido groups.

3.4.2. Pulse reaction with C_3H_6 in steady-state NO/O_2 flow. A progressive reaction of surface NO_x(ads) species was performed by pulse method to examine the behavior of surface species. After the formation of these species, five consecutive pulses of C_3H_6 were injected into the steady-state flow of NO/O_2/Ar over Ga_2O_3–Al_2O_3 at 573, 623, 673, and 723 K. Very similar IR spectra were obtained independently from reaction temperatures. The appearance of IR bands assignable to formate, acetate, –CN, –NCO, and –NH compounds was observed after the exposure of NO_x(ads) species to C_3H_6 pulses. Figure 11 shows the time

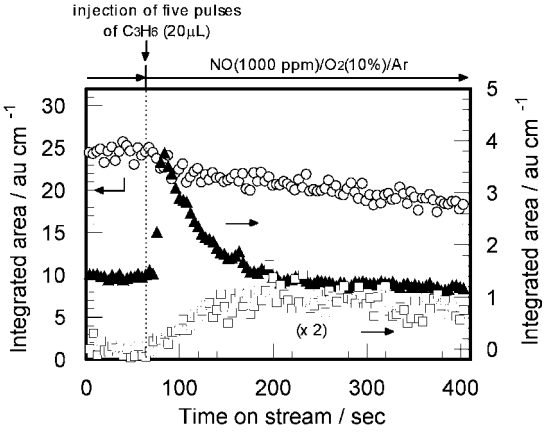

FIG. 11. Time dependence of the integrated area of the bands due to NO_x adspecies (○, NO_2^- and NO_3^-, 1175–1335 cm^{-1}), –NCO (▲, 2169–2325 cm^{-1}), and –NH (□, 3308–3463 cm^{-1}) species formed on the surface when introducing five consecutive pulses of C_3H_6 (1 pulse: 20 μL) into the steady-state flow of NO (1000 ppm)/O_2 (10%)/Ar on Ga_2O_3–Al_2O_3 at 623 K.

dependence of the integrated areas of IR bands due to surface species during the introduction of C_3H_6 pulses at 623 K. A slight decrease in the intensity of the IR bands due to NO_x(ads) species was observed with C_3H_6 pulsing. However, the decrease of the IR bands due to NO_x(ads) species was hardly recognized at higher temperatures (results not shown). This is probably because the formation of NO_x(ads) species was fast enough compared to its consumption. In accordance with the results obtained in the transient reaction described here, a quick formation rate of the –NCO species by C_3H_6 pulsing was observed, and then the –NCO species slowly vanished. No great difference in the formation rate of the –NCO species was observed at all reaction temperatures (results not shown), while their consumption rate increased with increasing reaction temperature. A decrease in the amount of –NCO species formed with the reaction temperature was also observed. It should be noted that a slow appearance of the IR bands due to adsorbed species including amido groups was recognized simultaneously with the decrease in –NCO species, although their surface concentration was quite low. The intensity of the ν(NH) bands gradually decreased after 250–300 s.

Figure 12 shows the time dependence of gaseous components measured by FT–IR and QMS during the introduction of C_3H_6 pulses at 623 K. It is understandable from the MS spectra (Fig. 12A) that C_3H_6 pulsing causes a consumption of NO ($m/e = 30$) and an evolution of N_2 and CO ($m/e = 28$) and N_2O and CO_2 ($m/e = 44$). In this case, since no considerable formation of CO and N_2O in the gas phase was recognized by FT–IR, the mass fragments of $m/e = 28$ and 44 were ascribed to N_2 and CO_2, respectively. A consumption of NO_x (NO + NO_2) by C_3H_6 pulsing was confirmed by FT–IR gas analysis (Fig. 12B). The big difference between the NO and NO_2 decrease can be ascribed to the different IR absorption coefficient: $\varepsilon(NO)/\varepsilon(NO_2) = 9/1$. In accordance with the reaction results described elsewhere (35), the NO_x consumption corresponding to NO_x conversion increased by increasing the reaction temperature.

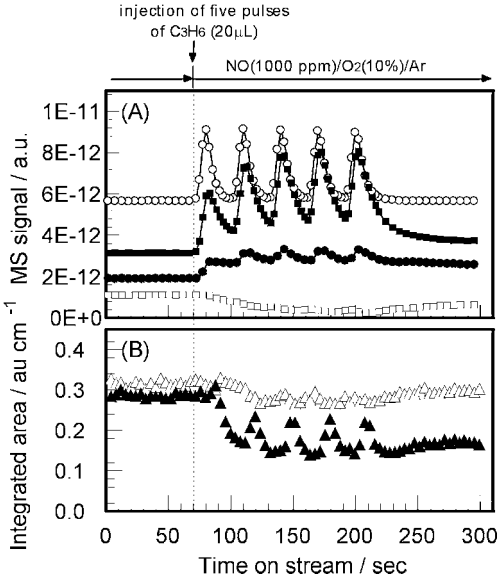

FIG. 12. (A) MS profiles of $m/e = 28$ (●, N_2 and/or CO), $m/e = 30$ (□, NO), $m/e = 41$ (○, C_3H_6) and $m/e = 44$ (■, CO_2 and/or N_2O) and (B) time dependence of the integrated area of the bands for NO (△, 1879–1958 cm^{-1}) and NO_2 (▲, 1563–1617 cm^{-1}) in the gas phase during five consecutive pulses of C_3H_6 (1 pulse: 20 μL) into the steady-state flow of NO (1000 ppm)/O_2 (10%)/Ar on Ga_2O_3–Al_2O_3 at 623 K.

4. DISCUSSION

The selective reduction of NO with hydrocarbons is a very complex reaction concerning several parallel and/or consecutive reaction steps. As the presence of oxygen is essential for NO reduction (54), oxygen contributes to several reaction steps. In this respect, the model, in which the initial step is the oxidation of NO to NO_2, is widely accepted. In addition, NO_x(ads) species such as nitrosonium ions (NO^+) (34, 53, 55), nitrates (NO_3^-) (21–25, 56), and nitrite (–ONO) (22, 56) have also been proposed to act as reaction initiators. In the present work, the formation of bidentate NO_3^- species was observed after an induction period of ca. 30 min in the NO–C_3H_6–O_2 reaction over Ga_2O_3–Al_2O_3 at 623 K, while no induction period was observed for C_3H_6-derived species such as acetates and formates (Fig. 4). This fact may be explained by the following considerations: the formation and adsorption of NO_x and another species competitively occur on the same sites. In the initial stage of the reaction, the consumption rate of NO_x(ads) species is much higher than the formation rate, and the formation of acetate and formates as products is predominant. The formation rate of NO_x(ads) species increases with the passage of time, resulting in their accumulation on the surface. This consideration is also supported by our previous steady-state kinetic studies that revealed the zero-order kinetics for NO in the formation of N_2 on Ga_2O_3–Al_2O_3, suggesting the direct participation of surface NO_x species (35).

As shown in Fig. 7, NO_x(ads) species (NO_2^- and NO_3^-) formed on Al_2O_3 and Ga_2O_3–Al_2O_3 were found to be highly reactive toward C_3H_6, leading to the formation of N_2 and CO_x (Fig. 8). From the results of the transient reaction given in Figs. 8 and 9, it was also deduced that the formation of N_2 and CO_x over Ga_2O_3–Al_2O_3 proceeded through a consecutive reaction via several surface species such as –CN and –NCO. Therefore, we considered that the reaction began with the formation of NO_x(ads) species via NO oxidation by O_2. The yield of N_2 and CO_x over Ga_2O_3–Al_2O_3 was much larger than that on Al_2O_3 (Fig. 8), whereas the consumption rate of NO_3^- species by the reaction with C_3H_6 over Al_2O_3 was very similar to that over Ga_2O_3–Al_2O_3 (Fig. 7). The presence of Ga_2O_3 seems to promote

the formation of important intermediates leading to N_2 formation, although the formation, accumulation, and subsequent reaction of NO_x(ads) species probably occur mainly on Al_2O_3.

Recently, Shimizu *et al.* (24, 26) emphasized the importance of acetate species, in addition to nitrate species, in the formation of N_2 on Al_2O_3. Although a certain amount of N_2 was formed by the reaction of oxygenate species and NO/O_2 (Fig. 6), the amount was much lower than that in the reaction of NO_x(ads) and C_3H_6 (Fig. 8). In this case, the main product was CO_x ($CO + CO_2$). It seems that acetate and formate species formed on Ga_2O_3–Al_2O_3 do not act as true intermediates leading to N_2 formation, as shown in their tendency to accumulate on the surface with time on stream (Fig. 4). They are probably mild oxidation products, which will be finally transformed to CO_x and H_2O. Since no great difference in the yields of N_2 and CO_x was observed between Al_2O_3 and Ga_2O_3–Al_2O_3 (Fig. 6), this reaction proceeded mainly on Al_2O_3. The hypothetical reaction pathway of NO reduction by propene over Ga_2O_3–Al_2O_3 is illustrated in Fig. 13.

A reaction step in which organic nitro (R-NO_2) and nitrite (R′-ONO) compounds are formed by the reaction between NO_x and hydrocarbons was proposed by many researchers (16, 18, 19, 57). For instance, Hayes *et al.* (58) proposed the reaction step in which organic nitro compounds are formed through the reaction of π-allyl and NO_2 during the NO reduction by propene over Cu-ZSM-5. In the present work, the reaction of NO_x(ads) and C_3H_6 gives rise to the appearance of the $\nu(CH_2)$ band (3094 cm^{-1}), suggesting the formation of acrylic species (Fig. 9). Since no IR band at 3094 cm^{-1} was observed during the NO–C_3H_6–O_2 reaction under steady-state conditions (Figs. 3 and 4), acrylic species may be capable of easily reacting with NO_x to form organic nitro compounds. However, organic nitro compounds are thermally unstable (20), so that the detection of the corresponding compounds by FT–IR is very difficult. Recently, we revealed the participation of organic nitro compounds such as 2-nitropropane in NO reduction by propene over Ga_2O_3–Al_2O_3 from the comparison of the distribution of minor products in the NO–C_3H_6–O_2 reaction and the 2-nitropropane oxidation (59). Therefore, organic nitro compounds could be formed through the reaction of NO_x(ads) species with propene.

In previous IR studies, the formation of –CN and –NCO species was reported for several kinds of catalysts (23, 27–33, 43–45, 49–53). As for their formation routes, Chen *et al.* (20) reported that decomposition of 2-nitropropane over Fe/ZSM-5 at 473 K formed a deposit including "CN" groups on the catalyst. On the other hand, Poignant *et al.* (33) proposed that the formation of –NCO species on Cu-ZSM-5 occured through the oxidation of isocyanide (–NC) species formed by the isomerization of –CN species. In the present work, –CN and –NCO species were formed immediately after the reaction of NO_x(ads) and C_3H_6, but the formation rate of the –NCO species was faster than that of the –CN species (Figs. 9 and 10). These facts suggest that the –CN and –NCO species are formed through alternative routes on this catalyst, leading to the consideration that the reaction step proposed by Poignant *et al.* (33) would be excluded in the present case. The formation of –CN and –NCO species would occur from the decomposition of organic nitro compounds. It should be noted that the reaction leading to the formation of –CN and –NCO species consists of very fast steps and that these steps are effectively promoted by the presence of Ga_2O_3.

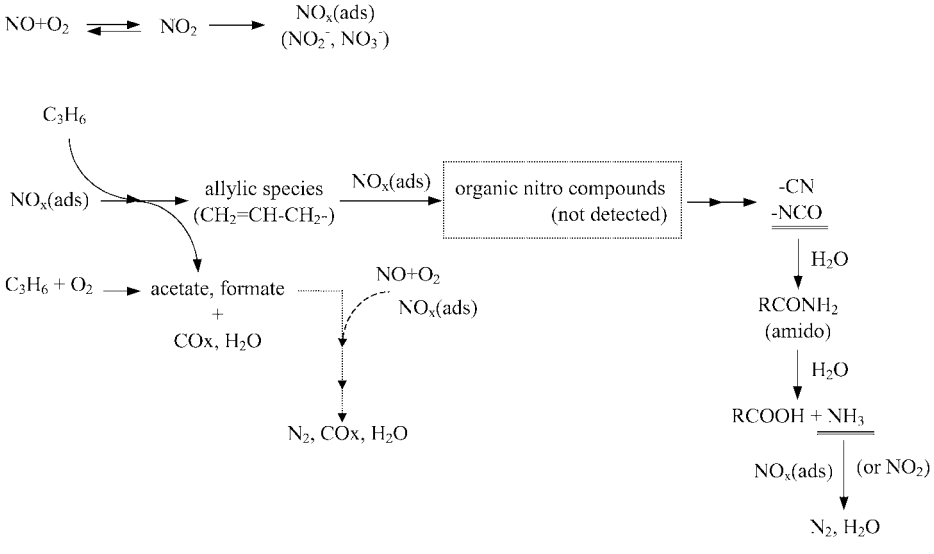

FIG. 13. Proposed reaction pathway of NO reduction by propene over Ga_2O_3–Al_2O_3.

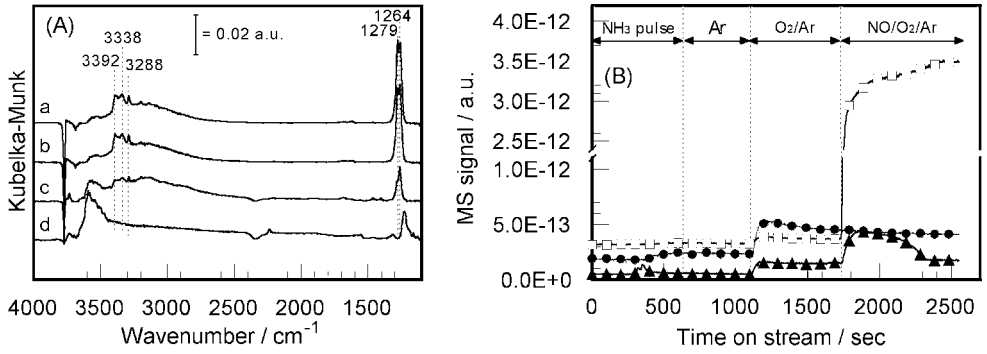

FIG. 14. (A) Diffuse reflectance FT–IR spectra of adsorbed species on Ga_2O_3–Al_2O_3 taken after pulsing NH_3 (20 μL) into a flow of Ar at 623 K, followed by (a) Ar purge for 10 min, (b) adding O_2 (10%) into Ar for 10 min, (c) adding NO (1000 ppm) into O_2 (10%)/Ar for 5 min, and (d) 10 min. (B) MS profiles of $m/e = 17$ (●, NH_3), $m/e = 28$ (▲, N_2), and $m/e = 30$ (□, NO) taken during the reaction of NH_3 adspecies with O_2 (10%)/Ar or NO (1000 ppm)/O_2 (10%)/Ar.

Many researchers (27–31) reported that –NCO species acted as the final intermediates leading to the formation of N_2. The –CN and –NCO species are also considered to be easily hydrolyzed to ammonia (including amines) and CO_2 if water is present in the gas phase and/or on the catalyst surface (32, 34, 60–62). In the present work, a strong band, (at around 3500 cm^{-1}), assigned to adsorbed water belonging to hydrocarbon combustion, was observed when several reactions were carried out, suggesting the possibility that the hydrolysis of –CN and –NCO species to ammonia and amines takes place. In fact, weak but distinct IR bands assignable to the N–H stretching vibrations (probably due to acrylamide species as mentioned earlier) were detected by the reaction of NO_x(ads) species with C_3H_6 (Fig. 9). Recently, Daturi and Saussey proposed the participation of acrylamide as an intermediate for the SCR mechanism on Cu-ZSM-5 (47). In the present work, the ν(NH) bands formed by the reaction of NO_x(ads) and C_3H_6 increased with time on stream and then gradually decreased after 250-300 s in the steady-state flow of NO/O_2/Ar (Fig. 11), suggesting that –NH compounds can react with NO_x (NO and/or NO_2). Hence, the reactivity of –NH compounds toward NO_x was evaluated at 623 K. In this experiment, NH_3 was employed as an –NH compound, because acrylamide is easily hydrolyzed to ammonia and carboxylic acid (47). After three consecutive pulses of NH_3 were injected into Ga_2O_3–Al_2O_3 to accumulate adsorbed NH_3 species on the surface, the reaction gas was switched to Ar, O_2/Ar, and NO/O_2/Ar. As shown in Fig. 14A, no changes in the IR bands due to adsorbed NH_3 species were observed in flowing Ar and O_2/Ar. Interestingly, the feature of IR bands due to adsorbed NH_3 species was gradually diminished by exposing the sample to NO/O_2/Ar flow (spectra c and d in Fig. 14A). Furthermore, a rapid evolution of N_2 was recognized in QMS signals (Fig. 14B). From these results, we can conclude that –NH compounds are capable of reacting with NO_x(ads) species and/or NO_2 leading to the formation of N_2.

5. CONCLUSIONS

The dynamic behavior of surface species formed during the selective reduction of NO with propene over Ga_2O_3–Al_2O_3 was investigated by using *in situ* diffuse reflectance FT–IR spectroscopy. The main surface species detectable by IR were nitrate (NO_3^-), acetate, formate, cyanide (–CN), and isocyanate (–NCO) during the steady–state reaction in flowing NO/C_3H_6/O_2/Ar. Transient and pulse reactions revealed that the selective reduction of NO with propene in the used temperature range could begin with the formation of NO_x(ads) species (NO_2^- and NO_3^-) by NO oxidation and their subsequent reaction with propene and/or propene-derived species to generate cyanide (–CN) and isocyanate (–NCO) species. On the other hand, acetate and formate species formed by mild oxidation of C_3H_6 were spectator species in the present reaction. The –NCO species are hydrolyzed to –NH compounds by reacting with the water present in the stream; then –NH compounds react with NO_x(ads) species and/or NO_2 to produce N_2. The hypothesized reaction pathway was applied to adsorbed NO_x(ads) species, so that *it could provide* precious information about the SCR mechanism for NO_x-trap catalysts.

ACKNOWLEDGMENTS

This work was carried out in the framework program with scientific collaboration between France and Japan (PICS France–Japan). M. Haneda gratefully acknowledges the financial support of the Centre National de la Recherche Scientifique (CNRS), France.

REFERENCES

1. Held, W., König, A., Richter, T., and Puppe, L., SAE Paper, 900496 (1990).
2. Iwamoto, M., Yahiro, H., Yu-u, Y., Sundo, S., and Mizuno, N., *Shokubai (Catalyst)* **32**, 430 (1990).
3. Iwamoto, M., and Yahiro, H., *Catal. Today* **22**, 5 (1994).
4. Misono, M., *CATTECH* **2**, 53 (1998).

5. Kikuchi, E., and Yogo, K., *Catal. Today* **22**, 73 (1994).
6. Burch, R., and Scire, S., *Appl. Catal. B* **3**, 295 (1994).
7. Armor, J. N., *Catal. Today* **31**, 191 (1996).
8. Chen, H.-Y., Wang, C., and Sachtler, W. M. H., *Appl. Catal. A* **194/195**, 159 (2000).
9. Fritz, A., and Pitchon, V., *Appl. Catal. B* **13**, 1 (1997).
10. Amiridis, M. A., Zhang, T., and Farrauto, R. J., *Appl. Catal. B* **10**, 203 (1996).
11. Hamada, H., *Catal. Today* **22**, 21 (1994).
12. Kung, M. C., and Kung, H. H., *Top. Catal.* **10**, 21 (2000).
13. Miyadera, T., and Yoshida, K., *Chem. Lett.* 1486 (1993).
14. Bethke, K. A., Kung, M. C., Yang, B., Shah, M., Alt, D., Li, C., and Kung, H. H., *Catal. Today* **26**, 169 (1995).
15. Zhang, X., Walters, A. B., and Vannice, M. A., *J. Catal.* **155**, 290 (1995).
16. Yokoyama, C., and Misono, M., *J. Catal.* **150**, 9 (1994).
17. Bethke, K. A., Li, C., Kung, M. C., Yang, B., and Kung, H. H., *Catal. Lett.* **31**, 287 (1995).
18. Smits, R. H., and Iwasawa, Y., *Appl. Catal. B* **6**, L201 (1995).
19. Martens, J. A., Cauvel, A., Francis, A., Hermans, C., Jayat, F., Remy, M., Keung, M., Lievens, J., and Jacobs, P. A., *Angew. Chem. Int. Ed.* **37**, 1901 (1998).
20. Chen, H. Y., Voskoboinikov, T., and Sachtler, W. M. H., *J. Catal.* **186**, 91 (1999).
21. Satsuma, A., Enjoji, T., Shimizu, K., Sato, K., Yoshida, H., and Hattori, T., *J. Chem. Soc., Faraday Trans.* **94**, 301 (1998).
22. Meunier, F. C., Breen, J. P., Zuzaniuk, V., Olsson, M., and Ross, J. R. H., *J. Catal.* **187**, 493 (1999).
23. Kameoka, S., Ukisu, Y., and Miyadera, T., *Phys. Chem. Chem. Phys.* **2**, 367 (2000).
24. Shimizu, K., Kawabata, H., Satsuma, A., and Hattori, T., *J. Phys. Chem. B* **103**, 5240 (1999).
25. Shimizu, K., Kawabata, H., Maeshima, H., Satsuma, A., and Hattori, T., *J. Phys. Chem. B* **104**, 2885 (2000).
26. Shimizu, K., Kawabata, H., Satsuma, A., and Hattori, T., *Appl. Catal. B* **19**, L87 (1998).
27. Ukisu, Y., Sato, S., Abe, A., and Yoshida, K., *Appl. Catal. B* **2**, 147 (1993).
28. Sumiya, S., He, H., Abe, A., Takezawa, N., and Yoshida, K., *J. Chem. Soc., Faraday Trans.* **94**, 2217 (1998).
29. Okuhara, T., Hasada, Y., and Misono, M., *Catal. Today* **35**, 83 (1997).
30. Iwamoto, M., and Takeda, H., *Catal. Today* **27**, 71 (1996).
31. Haneda, M., Kintaichi, Y., Inaba, M., and Hamada, H., *Catal.Today* **42**, 127 (1998).
32. Poignant, F., Saussey, J., Lavalley, J. C., and Mabilon, G., *J. Chem. Soc., Chem. Commun.* 89 (1995).
33. Poignant, F., Saussey, J., Lavalley, J. C., and Mabilon, G., *Catal. Today* **29**, 93 (1996).
34. Gerlach, T., Schütze, F. W., and Baerns, M., *J. Catal.* **185**, 131 (1999).
35. Haneda, M., Kintaichi, Y., Shimada, H., and Hamada, H., *J. Catal.* **192**, 137 (2000).
36. Hadjiivanov, K. I., *Catal. Rev.–Sci. Eng.* **42**, 71 (2000).
37. Davydov, A. A., "Infrared Spectroscopy of Adsorbed Species on the Surface of Transition Metal Oxides." Wiley, New York, 1990.
38. Haneda, M., Joubert, E., Ménézo, J. C., Duprez, D., Barbier, J., Bion, N., Daturi, M., Saussey, J., Lavalley, J. C., and Hamada, H., *Phys. Chem. Chem. Phys.* **3**, 1366 (2001).
39. Najbar, J., and Eischens, R. P., "Proceedings, 9th International Congress on Catalysis, 1998" (M. J. Phillips and M. Ternan, Eds.), Vol. 3, p. 1434. Chem. Institute of Canada, Ottawa, 1988.
40. Chauvin, C., Saussey, J., Lavalley, J. C., Idriss, H., Hindermann, J., Kiennemann, A., Chaumette, P., and Courty, P., *J. Catal.* **121**, 56 (1990).
41. Solymosi, F., and Bansagi, T. *J. Catal.* **156**, 75 (1995).
42. Morterra, C., Zecchina, A., Coluccia, S., and Chiorino, A., *J. Chem. Soc., Faraday Trans. 1* **73**, 1544 (1979).
43. Yasuda, H., Miyamoto, T., and Misono, M., *Prepr. Pap–Am. Chem. Soc. Div. Pet. Chem.* **39**, 99 (1994).
44. Tanaka, T., Okuhara, T., and Misono, M., *Appl. Catal. B* **4**, L1 (1994).
45. Tabata, T., Ohtsuka, H., Kokitsu, M., and Okada, O., *Bull. Chem. Soc. Jpn.* **68**, 1905 (1995).
46. Bellamy, L. J., "The Infrared Spectra of Complex Molecules." Wiley, New York, 1958.
47. Poignant, F., Freysz, J. L., Daturi, M., and Saussey, J., *Catal. Today* **70**, 197 (2001).
48. Nakamoto, K., "Infrared and Raman Spectra of Inorganic and Coordination Compounds," 5th edition. Wiley–Interscience, New York, 1997.
49. Ukisu, Y., Miyadera, T., Abe, A., and Yoshida, K., *Catal. Lett.* **39**, 265 (1996).
50. Kameoka, S., Chafik, T., Ukisu, Y., and Miyadera, T., *Catal. Lett.* **55**, 211 (1998).
51. Bion, N., Saussey, J., Hedouin, C., Seguelong, T., and Daturi, M., *Phys. Chem. Chem. Phys.* **3**, 4811 (2001).
52. Bamwenda, G. R., Ogata, A., Obuchi, A., Oi, J., Mizuno, K., and Skrzypek, J., *Appl. Catal. B* **6**, 311 (1995).
53. Hadjiivanov, K., Knözinger, H., Tsyntsarski, B., and Dimitrov, L., *Catal. Lett.* **62**, 35 (1999).
54. Iwamoto, M., Yahiro, H., Shundo, S., Yu-u, Y., and Miuno, N., *Appl. Catal.* **69**, L15 (1991).
55. Hadjiivanov, K., Saussey, J., Freysz, J. L., and Lavalley, J. C., *Catal. Lett.* **52**, 103 (1998).
56. Lobree, L. J., Hwang, I.-C., Reimer, J. A., and Bell, A. T., *Catal. Lett.* **63**, 223 (1999).
57. Djonev, B., Tsyntsarski, B., Klissurski, D., and Hadjiivanov, K., *J. Chem. Soc., Faraday Trans.* **93**, 4055 (1997).
58. Hayes, N. W., Joyner, R. W., and Shpiro, E. S., *Appl. Catal. B* **8**, 343 (1996).
59. Haneda, M., Joubert, E., Ménézo, J. C., Duprez, D., Barbier, J., Bion, N., Daturi, M., Saussey, J., Lavalley, J. C., and Hamada, H., *J. Mol. Catal. A*. **175**, 179 (2001).
60. Poignant, F., Freysz, J. L., Daturi, M., Saussey, J., and Lavalley, J. C., *Stud. Surf. Sci. Catal.* **130**, 1487 (2000).
61. Gerlach, T., Illgen, U., Bartoszek, M., and Baerns, M., *Appl. Catal. B* **22**, 269 (1999).
62. Nanba, T., Obuchi, A., Akaratiwa, S., Liu, S., Uchisawa, J., and Kushiyama, S., *Chem. Lett.* 986 (2000).